

# Hadronic three-body decays of light vector mesons

S. Leupold<sup>1</sup> and M.F.M. Lutz<sup>2</sup>

<sup>1</sup> Institut für Theoretische Physik, Johann Wolfgang Goethe-Universität Frankfurt, Germany

<sup>2</sup> GSI, Planckstrasse 1, D-64291 Darmstadt, Germany

July 29, 2008

**Abstract.** The decays of light vector mesons into three pseudoscalar mesons are calculated to leading order in the recently proposed counting scheme that is based on the hadrogenesis conjecture. Fully differential as well as integrated decay widths are presented. Since the required parameters have been fixed by other processes, the considered three-body decays are predictions of the presented approach. The decay width of the omega meson into three pions agrees very well with experiment. The partial decay widths of the  $K^*$  into its three  $K\pi\pi$  channels are predicted.

## 1 Introduction

One of the open challenges of QCD is to develop a systematic scheme for the calculation of hadronic reactions and decays. In the sector of mesons made out of light quarks, chiral perturbation theory [1,2] provides such a systematic approach. However, it is restricted to energies where no other mesons than the Goldstone bosons participate as active degrees of freedom. It is therefore important to construct effective field theories with additional degrees of freedom. In particular, in the framework of the hadrogenesis conjecture [3] such an extension is mandatory since the pseudoscalar and vector mesons together with the baryon octet and decuplet are regarded as the preselected states which build up the other hadrons — at least in the low-energy regime.

Recently we have suggested in [4] a counting scheme for flavor-SU(3) systems of Goldstone bosons and light vector mesons. The quest is to have a scheme at hand which allows in particular for decays of vector mesons into pseudoscalar states. The masses of pseudoscalar ( $P$ ) and vector mesons ( $V$ ) and all involved momenta are treated as soft, i.e.  $m_P, m_V \sim Q$ , where  $Q$  is a typical momentum. Such an assumption may be justified in QCD with a large number of colors  $N_c$ , which implies that the chiral symmetry breaking scale is much larger than the vector meson masses, i.e.  $4\pi f_\pi \gg m_V$ . Consequently, all chirally covariant derivatives  $D_\mu$  are  $\sim Q$ , no matter whether they act on pseudoscalar or vector mesons. This is in contrast to the approach where vector mesons are treated as heavy matter fields [5]. The latter formalism does not allow for a systematic treatment of processes where the number of vector mesons changes, like e.g. in vector-meson decays. Our scheme is also different from the one presented in [6,7] where all derivatives are treated as soft, but the masses of the vector mesons are treated as heavy. Strictly speaking, such an approach is restricted to energies below the vector

meson masses. Nonetheless, resonance saturation models based on large- $N_c$  considerations have been built upon the works [6,7] and have been applied also to processes at higher energies, see e.g. [8] and references therein.

For the present purpose it is only important to recall from [4] that loops are suppressed which is a generic consequence of large- $N_c$  considerations [9]. It is important to note that the vector mesons are represented by tensor fields in our approach. The chosen representation cannot change the physical results, but contact terms (e.g. four-point interactions) can look different in different representations and different orders in a given counting scheme might be attributed to them.

It has been demonstrated in [4] that the proposed scheme can be used to describe hadronic and electromagnetic two-body decays of vector mesons. In the present work we explore some further consequences of this framework by calculating to leading order the decays of vector mesons into three pseudoscalar mesons. It will turn out that all necessary parameters for the leading-order calculation have already been determined from the two-body decays. Therefore, our calculations can be tested against the available experimental data and we can provide predictions for processes which were not measured yet or not measured in a fully differential way.

In the following we will study the process  $\omega \rightarrow 3\pi$  and the three decay branches of  $K^* \rightarrow K\pi\pi$ . There are no data for any differential widths of these three-body decays available. The partial decay width for the omega decay is measured [10] whereas for the  $K^*$  decays only upper limits exist [11]. The omega decay has been studied by several groups, see e.g. [12] and references therein. Typically, however, the corresponding coupling constants have been fitted to the partial decay width of the process  $\omega \rightarrow 3\pi$ . In our approach we have determined the required coupling constants from two-body processes and we have a counting scheme which tells us that we have covered

all relevant vertices. An approach which is on the technical level close to ours is the one presented in [8]. Also there tensor fields have been used to represent the vector mesons. However, the counting scheme is different since vector meson masses are treated as heavy in [8]. Therefore, also the results cannot be compared easily. For the decays of the  $K^*$  the literature is scarce. In [13] various models including vector-meson dominance and also contact interactions (see discussion below in sect. 2) have been applied to the three-body decays of the  $K^*$ . We will comment on the work of [13] when we present our results below. In contrast to previous works differential decay widths for the considered processes will be presented. To the best of our knowledge this issue has not been studied at all by other theory groups.

The work is structured in the following way: In the next section we present the relevant part of our leading-order Lagrangian and provide some general formulae important for three-body decays. In sect. 3 we calculate the decay of the omega meson into three pions. We will present the fully differential decay width (Dalitz plot) as well as integrated quantities thereof. The corresponding calculations for the decay channels of the  $K^*$  into one kaon and two pions are presented in sect. 4. Finally in sect. 5 we summarize our results.

## 2 Three-body decays

We compute the decays of light vector mesons into three pseudoscalar mesons. In general, such a calculation involves (a) tree diagrams with three-point vertices, (b) a tree diagram with a four-point vertex and (c) loops. We shall show now that only case (a) is relevant at leading order in the scheme proposed in [4]: For the considered decays the leading-order calculation is of second order. Loops are suppressed contributing at fourth order [4]. In principle, it is conceivable that a four-point vertex with one vector and three pseudoscalar states could enter at leading, i.e. second, order. However, within the tensor representation, which we use, one needs at least four derivatives to construct such a vertex. Thus it has at least order four according to the counting rules of [4]. Hence at the leading-order calculation, on which we concentrate in the following, one only needs three-point vertices. Since a three-point vertex with three pseudoscalar states does not exist, the decay process happens in two steps: The initial vector meson decays into another vector meson and one pseudoscalar state. The emerging vector meson finally decays into two pseudoscalar states. The generic diagram is depicted in fig. 1.

We recall from [4] the relevant part of the leading-order Lagrangian:

$$\begin{aligned} \mathcal{L} = & -\frac{h_A}{16f} \epsilon^{\mu\nu\alpha\beta} \text{tr} \{ (V_{\mu\nu} (\partial^\tau V_{\tau\alpha}) + (\partial^\tau V_{\tau\alpha}) V_{\mu\nu}) \partial_\beta \Phi \} \\ & + i \frac{m_V h_P}{8f^2} \text{tr} \{ V^{\mu\nu} \partial_\mu \Phi \partial_\nu \Phi \} \\ & - \frac{b_A}{16f} \epsilon^{\mu\nu\alpha\beta} \text{tr} \left\{ [V_{\mu\nu}, V_{\alpha\beta}]_+ [\Phi, \chi_0]_+ \right\}. \end{aligned} \quad (1)$$

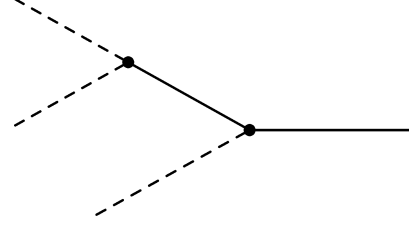


**Fig. 1.** Feynman diagram which contributes in leading order to the decay of a vector meson (solid line) into three pseudoscalar mesons (dashed lines).

with the conventions

$$V_{\mu\nu} = \begin{pmatrix} \rho_{\mu\nu}^0 + \omega_{\mu\nu} & \sqrt{2} \rho_{\mu\nu}^+ & \sqrt{2} K_{\mu\nu}^+ \\ \sqrt{2} \rho_{\mu\nu}^- & -\rho_{\mu\nu}^0 + \omega_{\mu\nu} & \sqrt{2} K_{\mu\nu}^0 \\ \sqrt{2} K_{\mu\nu}^- & \sqrt{2} \bar{K}_{\mu\nu}^0 & \sqrt{2} \phi_{\mu\nu} \end{pmatrix}, \quad (2)$$

$$\Phi = \begin{pmatrix} \pi^0 + \frac{1}{\sqrt{3}} \eta & \sqrt{2} \pi^+ & \sqrt{2} K^+ \\ \sqrt{2} \pi^- & -\pi^0 + \frac{1}{\sqrt{3}} \eta & \sqrt{2} K^0 \\ \sqrt{2} K^- & \sqrt{2} \bar{K}^0 & -\frac{2}{\sqrt{3}} \eta \end{pmatrix}, \quad (3)$$

$$\chi_0 = \begin{pmatrix} m_\pi^2 & 0 & 0 \\ 0 & m_\pi^2 & 0 \\ 0 & 0 & 2m_K^2 - m_\pi^2 \end{pmatrix}. \quad (4)$$

In (1) the quantity  $f$  denotes the pion-decay constant in the chiral limit. The quantity  $m_V$  has been introduced for convenience to render the coupling constants in (1) dimensionless. The combination  $m_V h_P / f^2$  has been fixed in [4] from the decays of vector mesons into two pseudoscalar states. The leading-order Lagrangian of our approach has only one such term. Hence it predicts a universal value for the coupling constant for all these decays, i.e. for  $\rho \rightarrow 2\pi$ ,  $K^* \rightarrow \pi K$  and  $\phi \rightarrow K \bar{K}$ . Indeed, the values for  $h_P$  obtained from fits to the experimental decay widths agree with each other within  $\pm 10\%$ . The values for  $h_A$  and  $b_A$  have been determined from the radiative decays of vector mesons [4]. Here, it turned out that one universal vertex would be insufficient to describe all the radiative two-body decays of the vector meson nonet. Indeed, our leading-order Lagrangian yields two terms — one flavor symmetric, one flavor breaking — which are then sufficient to describe the data [4]. We regard this as a support of our approach.

The only decays which are allowed by energy-momentum conservation and where our Lagrangian yields non-vanishing couplings at leading order are  $\omega \rightarrow 3\pi$  and  $K^* \rightarrow 2\pi + K$ . Note that in leading order the  $\phi$  is purely strange and OZI suppression [14, 15, 16] is perfect. Hence we do not provide results for the OZI suppressed decay branch  $\phi \rightarrow 3\pi$ .

In the following we use the values

$$\begin{aligned} f &= 90 \text{ MeV}, \quad m_V = 776 \text{ MeV}, \\ h_P &= 0.304, \quad h_A = 2.1, \quad b_A = 0.27. \end{aligned} \quad (5)$$

Note that the precise value for  $h_P$  emerges from a fit to the electromagnetic pion form factor [17]. For the two-body decay of the  $K^*$  this value for  $h_P$  implies a partial width of 50.9 MeV, in excellent agreement with data [10].

In [4] we have deduced for  $h_P$  a value of  $0.29 \pm 0.03$  which agrees with the one given in (5) within the error bars. This result of [4] emerged from a simultaneous fit to the decay widths  $\rho \rightarrow \pi\pi$ ,  $K^* \rightarrow K\pi$  and  $\phi \rightarrow K\bar{K}$ . For the processes of interest in the present context the  $\phi$  decay does not enter. Hence we use a value for  $h_P$  which agrees well with the processes  $\rho \rightarrow \pi\pi$  and  $K^* \rightarrow K\pi$  relevant for the decay chains depicted in fig. 1.

We consider the decay of a state  $V$  with momentum  $p$  into three states with momenta  $p_1$ ,  $p_2$  and  $p_3$ . According to [10] the double differential decay rate

$$\frac{d^2\Gamma_{V \rightarrow 123}}{dm_{12}^2 dm_{23}^2} = \frac{1}{(2\pi)^3} \frac{P}{32 M^3} |C_{V \rightarrow 123}|^2, \quad (6)$$

$$P = -\frac{1}{3} \epsilon_{\mu\nu\alpha\beta} p^\mu p_1^\nu p_2^\alpha \epsilon_{\bar{\mu}\bar{\nu}\bar{\alpha}\bar{\beta}} p^{\bar{\mu}} p_1^{\bar{\nu}} p_2^{\bar{\alpha}},$$

is determined by a matrix element  $C_{V \rightarrow 123}$  and the phase-space factor  $P$ . In (6) we introduced the following variables

$$\begin{aligned} m_{ij}^2 &= (p_i + p_j)^2, & M^2 &= p^2, \\ q_1^2 &= m_{23}^2, & q_3^2 &= m_{12}^2, \\ q_2^2 &= m_{13}^2 = p^2 - m_{12}^2 - m_{23}^2 + p_1^2 + p_2^2 + p_3^2. \end{aligned} \quad (7)$$

The additional quantities  $q_i^2$  are introduced for later convenience.

### 3 Decay $\omega \rightarrow 3\pi$

The differential decay width of the process  $\omega \rightarrow \pi^+ \pi^- \pi^0$  is determined by the matrix element

$$\begin{aligned} C_{\omega \rightarrow \pi^+ \pi^- \pi^0} &= \frac{m_V h_P h_A}{4 f^3 m_\omega} [S_\rho(q_1^2)(q_1^2 + m_\omega^2) \\ &\quad + S_\rho(q_2^2)(q_2^2 + m_\omega^2) + S_\rho(q_3^2)(q_3^2 + m_\omega^2)] \\ &\quad - \frac{2 m_V h_P m_\pi^2 b_A}{f^3 m_\omega} [S_\rho(q_1^2) + S_\rho(q_2^2) + S_\rho(q_3^2)], \end{aligned} \quad (8)$$

where we use the kinematics of (7). In (8) the rho-meson propagator

$$S_\rho(q^2) = \frac{1}{q^2 - m_\rho^2 + i\Gamma_\rho(q^2)} \quad (9)$$

appears. Here  $\Gamma_\rho(q^2)$  denotes the energy-dependent width of the rho meson. It turns out that the results only change by about 2%, if this width is neglected. We do not think that our leading-order calculation and the determination of our coupling constants have a comparable accuracy. Hence we refrain from a more detailed modeling of the rho-meson propagator including e.g. an energy dependent real part of the self energy.

The factors  $q_i^2 + m_\omega^2$  which accompany the rho-meson propagators in (8) emerge from the use of the tensor representation for the vector mesons. In other representations this combination might split up into contact terms and vector-meson exchange terms. In our approach we do not have extra contact terms in leading order and therefore

one parameter combination  $\sim h_P h_A$  determines the decay process, at least in the chiral limit. Quantitatively the extra term  $\sim m_\pi^2 b_A$  plays only a minor role.

In fig. 2 the Dalitz plot for the decay process  $\omega \rightarrow \pi^+ \pi^- \pi^0$  is depicted using the values (5). The shape can be compared with the one obtained from pure phase space, i.e. replacing  $C_{\omega \rightarrow \pi^+ \pi^- \pi^0}$  by a constant. A pure phase space Dalitz shape is shown in fig. 3. There are no visible differences and indeed in the kinematically allowed range the squared matrix element  $|C_{\omega \rightarrow \pi^+ \pi^- \pi^0}|^2$  is rather flat (not shown).

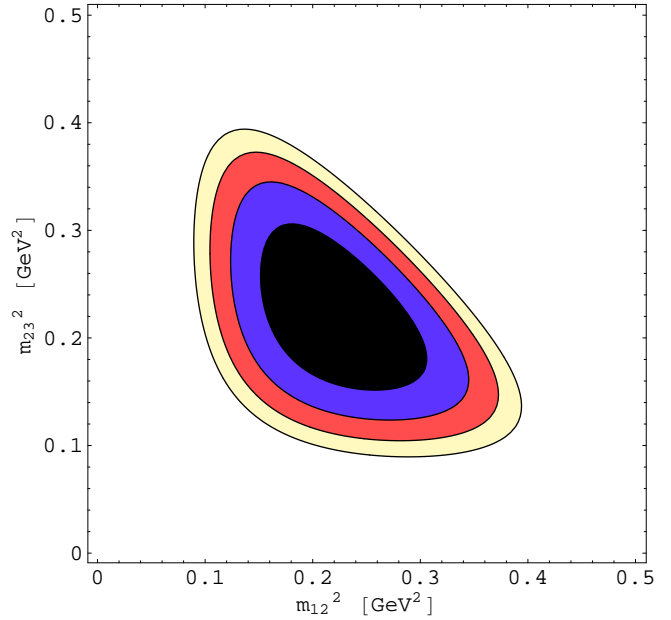


**Fig. 2.** Dalitz plot for the decay process  $\omega \rightarrow \pi^+ \pi^- \pi^0$  (arbitrary normalization). Note  $m_{12}^2 = m_{\pi^+ \pi^-}^2$  and  $m_{23}^2 = m_{\pi^- \pi^0}^2$ .

The single-differential decay width  $\frac{d\Gamma_{\omega \rightarrow 3\pi}}{dm_{12}^2}$  is plotted in fig. 4. One observes the typical rise and fall of phase space. We predict that the shape of the fully and single-differential decay widths do not differ significantly from pure phase space. It was checked that this finding emerges from the interference of the respective three rho-meson terms which appear in (8). Physically this corresponds to the three decays  $\omega \rightarrow \rho^+ \pi^-$ ,  $\omega \rightarrow \rho^0 \pi^0$ ,  $\omega \rightarrow \rho^- \pi^+$ . If there was only one rho meson, e.g. the  $\rho^+$ , the Dalitz shape would differ significantly from pure phase space.

For the partial decay width one gets

$$\Gamma_{\omega \rightarrow 3\pi} = 7.3 \text{ MeV} \quad (10)$$

which agrees very well with the experimental value [10]

$$\Gamma_{\omega \rightarrow 3\pi}^{\text{exp}} = (7.57 \pm 0.13) \text{ MeV}. \quad (11)$$

As stated before the influence of  $b_A$  is of minor importance here. Using  $b_A = 0$  leads to  $\Gamma_{\omega \rightarrow 3\pi} = 7.7 \text{ MeV}$ . We emphasize that our coupling constants have been obtained from

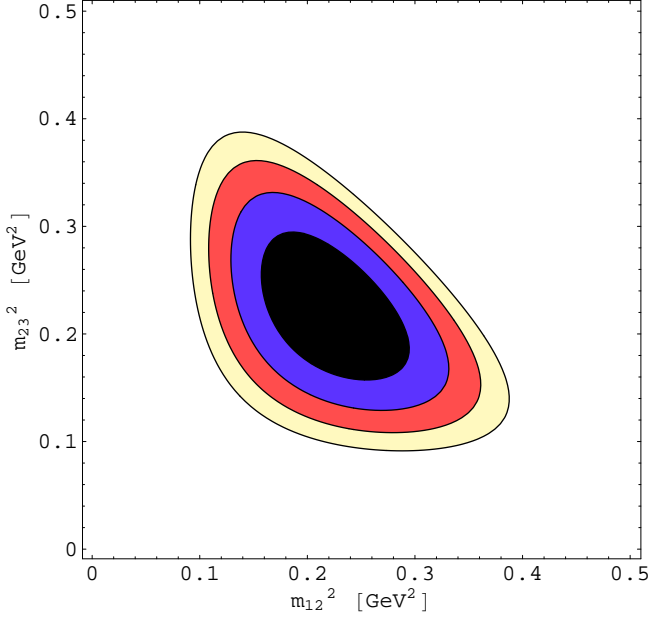


**Fig. 3.** Dalitz plot for the phase space of the decay process  $\omega \rightarrow \pi^+ \pi^- \pi^0$ .

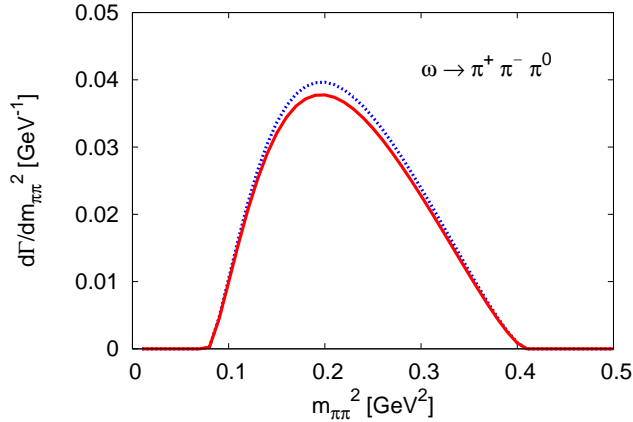


**Fig. 4.** Single-differential decay width for the process  $\omega \rightarrow \pi^+ \pi^- \pi^0$ . The solid line gives the full result, the dotted with  $b_A = 0$ .

other processes. Thus, the good agreement between (10) and (11) can be regarded as a further justification for our approach which predicts that the considered three-body decay processes are governed by vector-meson dominance (cf. fig. 1). We stress again that such a statement hinges on the representation used for the vector meson fields (cf. also the discussion in [7]). In our work we use tensor fields and our counting scheme leaves no room for contact terms at leading order. Other works, which use the vector representation, do find additional contact terms, see e.g. [12] and references therein. We stress again that in these works the experimental decay width (11) is used to pin down the coupling constants of the respective model. In contrast, our result (10) is a consequence of our effective Lagrangian

which connects in a systematic way the two-body decays studied in [4] with the three-body decays studied here.

#### 4 Decay $K^* \rightarrow K \pi \pi$

We turn to the decay modes of the  $K^{*+}$ . Due to isospin symmetry the decay modes of the  $K^{*0}$  need not be considered separately. Three decay channels exist:  $K^{*+} \rightarrow \pi^+ \pi^- K^+$ ,  $K^{*+} \rightarrow \pi^0 K^+ \pi^0$ ,  $K^{*+} \rightarrow \pi^+ K^0 \pi^0$ .

Let us first discuss the experimental situation: In [11] upper limits are given for the processes

$$\begin{aligned} \Gamma_{K^{*-} \rightarrow \pi^+ \pi^- K^-} &< 40 \text{ keV}, \\ \Gamma_{K^{*-} \rightarrow \pi^- \pi^0 \bar{K}^0} &< 35 \text{ keV}, \\ \Gamma_{\bar{K}^{*0} \rightarrow \pi^+ \pi^- \bar{K}^0} &< 35 \text{ keV}. \end{aligned} \quad (12)$$

Using particle-antiparticle symmetry and flipping the isospin for the latter process this yields the following constraints for the  $K^{*+}$  decays:

$$\begin{aligned} \Gamma_{K^{*+} \rightarrow \pi^+ \pi^- K^+} &< 40 \text{ keV}, \\ \Gamma_{K^{*+} \rightarrow \pi^+ \pi^0 K^0} &< 35 \text{ keV}, \\ \Gamma_{K^{*+} \rightarrow \pi^+ \pi^- K^+} &< 35 \text{ keV}. \end{aligned} \quad (13)$$

##### 4.1 Decay $K^{*+} \rightarrow \pi^+ \pi^- K^+$

We identify the three states with momenta  $p_1, p_2, p_3$  with  $\pi^+, \pi^-, K^+$ , respectively. The relevant matrix element to be used in (6) is

$$\begin{aligned} C_{K^{*+} \rightarrow \pi^+ \pi^- K^+} = & \\ \frac{m_V h_P h_A}{8 f^3 m_{K^*}} [S_\rho(q_3^2) (q_3^2 + m_{K^*}^2) + S_{K^*}(q_1^2) (q_1^2 + m_{K^*}^2)] & \\ - \frac{m_V h_P m_\pi^2 b_A}{f^3 m_{K^*}} \left[ \frac{m_K^2}{m_\pi^2} S_\rho(q_3^2) + S_{K^*}(q_1^2) \right]. & \end{aligned} \quad (14)$$

The propagator of the  $K^*$  meson is constructed in the same way as the rho-meson propagator (9). Also here it does not influence the results appreciably, if the energy dependent width of the  $K^*$  meson is neglected.

The Dalitz plot for this reaction is shown in fig. 5. The corresponding plot with pure phase space is depicted in fig. 6. There are some deviations from pure phase space which are interesting to be resolved experimentally.

The single-differential decay width  $\frac{d\Gamma_{K^{*+} \rightarrow \pi^+ \pi^- K^+}}{dm_{12}^2}$  is plotted in fig. 7. No significant deviations from pure phase space remain in this integrated quantity (not shown).

For the partial decay width one gets

$$\Gamma_{K^{*+} \rightarrow \pi^+ \pi^- K^+} = 14 \text{ keV}, \quad (15)$$

in agreement with the experimental constraints (13). Switching off the effect of  $b_A$  increases the width by 4 keV. The order of magnitude of our result (15) agrees with the range given in [13]. It clearly would be interesting to confront our prediction with experimental results. In high-statistics experiments like e.g. HADES at GSI and WASA at COSY it might be possible to observe such rare decays.

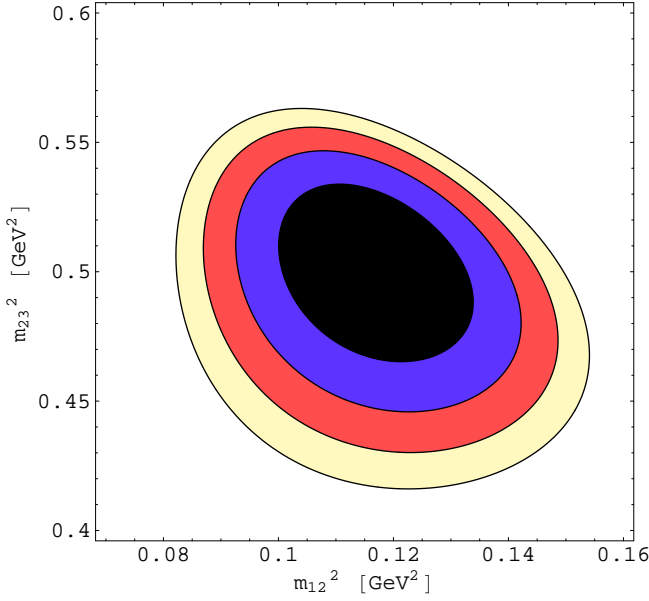


**Fig. 5.** Dalitz plot for the decay process  $K^{*+} \rightarrow \pi^+ \pi^- K^+$  (arbitrary normalization). Note  $m_{12}^2 = m_{\pi^+ \pi^-}^2$  and  $m_{23}^2 = m_{\pi^- K^+}^2$ .

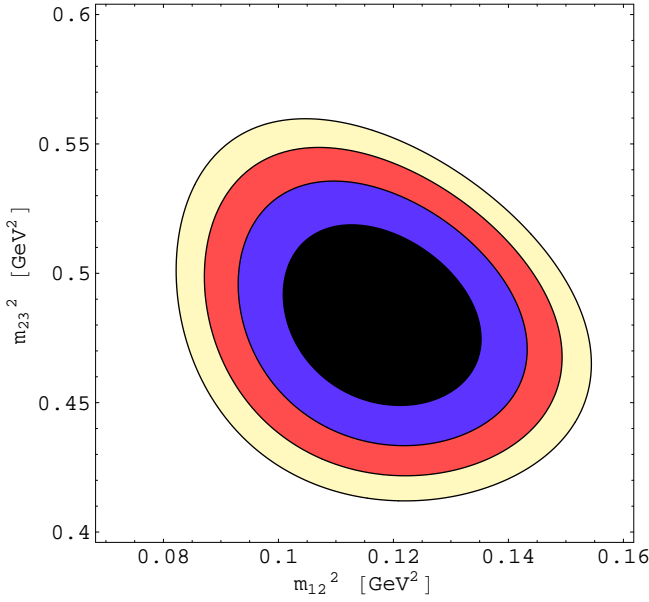


**Fig. 6.** Dalitz plot for the phase space of the decay process  $K^{*+} \rightarrow \pi^+ \pi^- K^+$ .

#### 4.2 Decay $K^{*+} \rightarrow \pi^0 K^+ \pi^0$

For the decay  $K^{*+} \rightarrow \pi^0 K^+ \pi^0$  we identify the three states 1, 2, 3 with  $\pi^0$ ,  $K^+$ ,  $\pi^0$ , respectively. It holds

$$C_{K^{*+} \rightarrow \pi^0 K^+ \pi^0} = \frac{m_V h_P h_A}{16 f^3 m_{K^*}} \times [S_{K^*}(q_3^2)(q_3^2 + m_{K^*}^2) - S_{K^*}(q_1^2)(q_1^2 + m_{K^*}^2)]$$

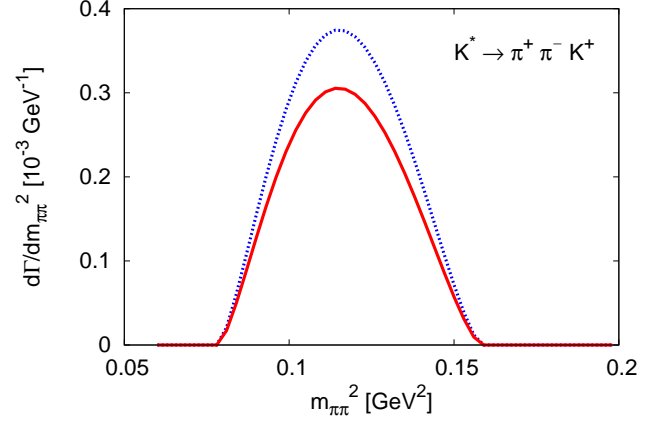


**Fig. 7.** Single-differential decay width for the process  $K^{*+} \rightarrow \pi^+ \pi^- K^+$ . The solid line gives the full result, the dotted with  $b_A = 0$ .

$$- \frac{m_V h_P m_\pi^2 b_A}{2 f^3 m_{K^*}} [S_{K^*}(q_3^2) - S_{K^*}(q_1^2)] . \quad (16)$$

In addition, for the decay width one has to account for the presence of two identical states by a factor  $1/2$ .

The Dalitz plot for this reaction is shown in fig. 8. Due to the destructive interference present in (16) there is a striking difference to pure phase space shown in fig. 9.

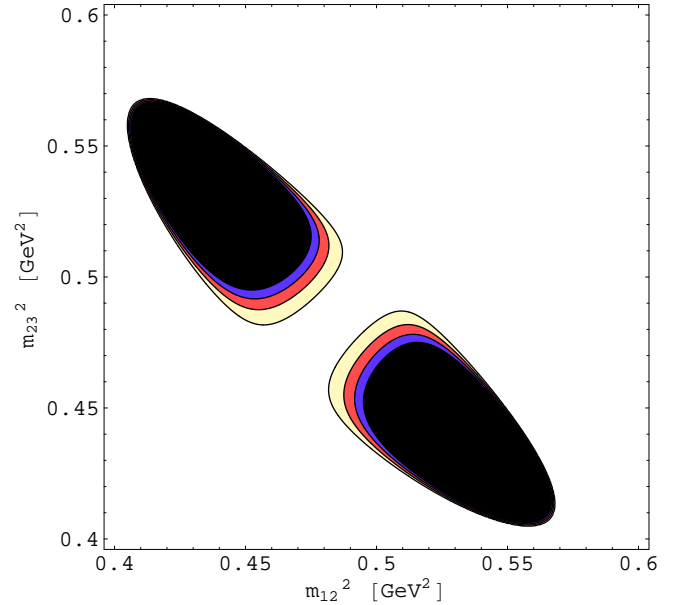


**Fig. 8.** Dalitz plot for the decay process  $K^{*+} \rightarrow \pi^0 K^+ \pi^0$  (arbitrary normalization). Note  $m_{12}^2 = m_{\pi^0 K^+}^2$  and  $m_{23}^2 = m_{K^+ \pi^0}^2$ .

The single-differential decay width  $\frac{d\Gamma_{K^{*+} \rightarrow \pi^0 K^+ \pi^0}}{dm_{12}^2}$  is plotted in fig. 10. Again the difference to pure phase space

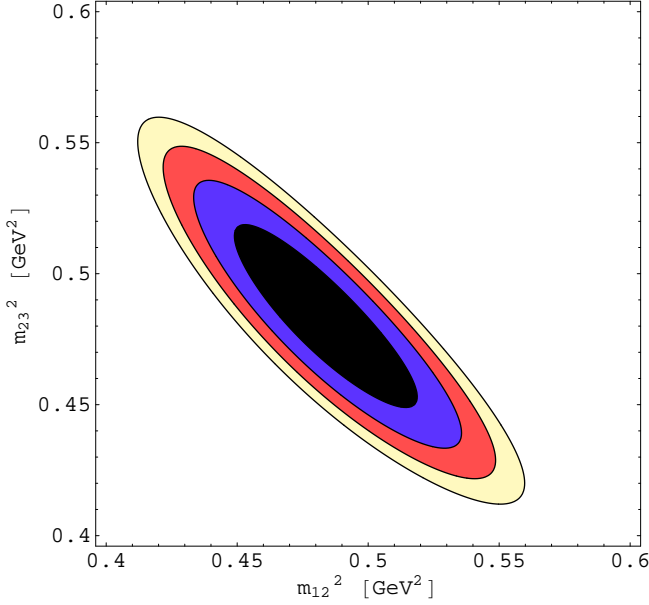


**Fig. 9.** Dalitz plot for the phase space of the decay process  $K^{*+} \rightarrow \pi^0 K^+ \pi^0$ .

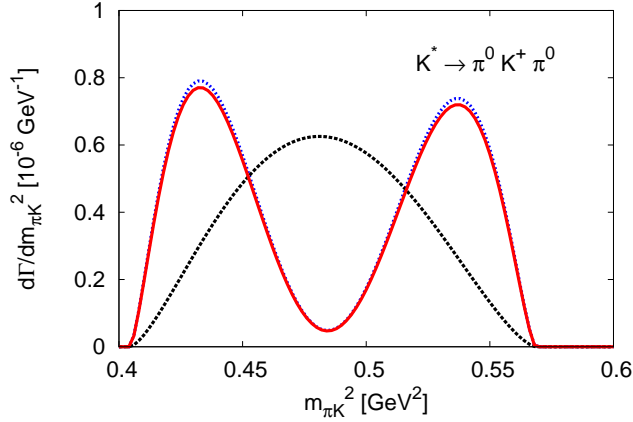


**Fig. 10.** Single-differential decay width for the process  $K^{*+} \rightarrow \pi^0 K^+ \pi^0$ . The solid line gives the full result, the dotted with  $b_A = 0$ . For comparison also the shape for pure phase space is plotted as the dashed line.

is obvious. For the partial decay width one gets the value

$$\Gamma_{K^{*+} \rightarrow \pi^0 K^+ \pi^0} = 67 \text{ eV}, \quad (17)$$

whereas  $b_A = 0$  leads to 69 eV. It has already been pointed out in [13] that this particular decay channel has a rather small width. Of course, this smallness is caused by the already mentioned negative interference. Hence, while a fully or single-differential width shows an interesting pattern, the overall missing strength of this decay channel probably inhibits an experimental verification.

### 4.3 Decay $K^{*+} \rightarrow \pi^+ K^0 \pi^0$

We identify the three states 1, 2, 3 in (6) with  $\pi^+$ ,  $K^0$ ,  $\pi^0$ , respectively and derive

$$\begin{aligned} C_{K^{*+} \rightarrow \pi^+ K^0 \pi^0} = & \frac{m_V h_P h_A}{8 \sqrt{2} f^3 m_{K^*}} [S_{K^*}(q_1^2)(q_1^2 + m_{K^*}^2) \\ & + S_{K^*}(q_3^2)(q_3^2 + m_{K^*}^2) + 2 S_\rho(q_2^2)(q_2^2 + m_{K^*}^2)] \\ & - \frac{m_V h_P m_\pi^2 b_A}{\sqrt{2} f^3 m_{K^*}} \left[ S_{K^*}(q_1^2) + S_{K^*}(q_3^2) + 2 \frac{m_K^2}{m_\pi^2} S_\rho(q_2^2) \right]. \end{aligned} \quad (18)$$

The Dalitz plot for this reaction is shown in fig. 11. In practice there is no difference to pure phase space shown in fig. 9.

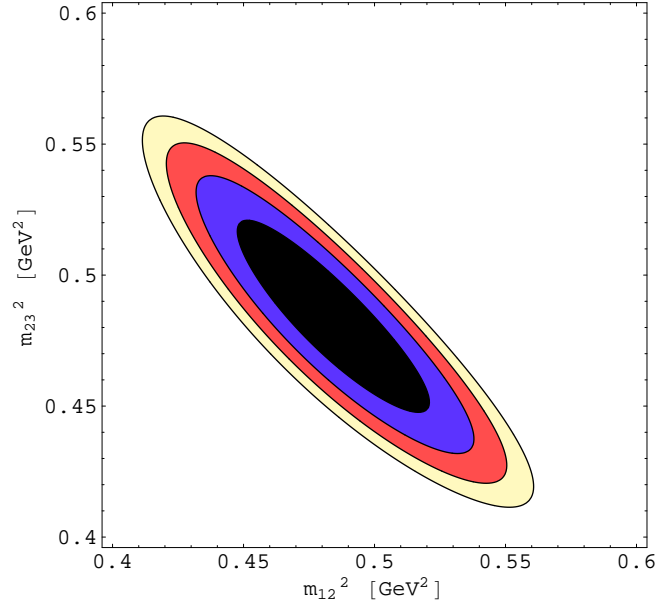


**Fig. 11.** Dalitz plot for the decay process  $K^{*+} \rightarrow \pi^+ K^0 \pi^0$  (arbitrary normalization). Note  $m_{12}^2 = m_{\pi^+ K^0}^2$  and  $m_{23}^2 = m_{K^0 \pi^0}^2$ .

The single-differential decay width  $\frac{d\Gamma_{K^{*+} \rightarrow \pi^+ K^0 \pi^0}}{dm_{12}^2}$  is plotted in fig. 12. For the partial decay width one gets

$$\Gamma_{K^{*+} \rightarrow \pi^+ K^0 \pi^0} = 28 \text{ keV}. \quad (19)$$

This result is in agreement with the experimental constraints (13). We observe that for this decay the influence of  $b_A$  is significant. For  $b_A = 0$  the decay width comes at 35 keV, right at the boundary of the empirical constraint (13). Qualitatively, also in [13] it was found that the decay width (19) is about twice as large as the one given in (15).

Among the three-body decay branches of the  $K^{*+}$  meson the partly charged channel  $\pi^+ K^0 \pi^0$  has the largest width. An experimental verification of our results (15),

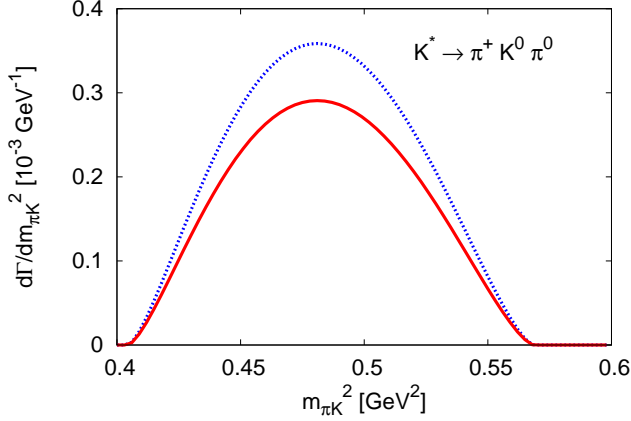


**Fig. 12.** Single-differential decay width for the process  $K^{*+} \rightarrow \pi^+ K^0 \pi^0$ . The solid line gives the full result, the dotted with  $b_A = 0$ .

(17), (19) for the partial widths and maybe even for the differential widths shown in figs. 5, 7, 8, 10, 11 and 12 would be highly desirable. Like in the radiative two-body decays studied in [4] we predict sizeable flavor breaking effects in the hadronic three-body decays.

## 5 Summary

The chiral Lagrangian with Goldstone bosons and light vector mesons has been used to calculate hadronic three-body decays of light vector mesons following the recently proposed counting rules [4]. The leading order results agree very well with all available data and constraints. We have presented predictions for differential decay widths of all considered processes and for the partial decay widths of the three-body decays of the  $K^*$  meson. We suggest to study such reactions in high-statistics experiments like HADES at GSI and WASA at COSY.

## References

1. J. Gasser, H. Leutwyler, Nucl. Phys. **B250**, 465 (1985)
2. S. Scherer, Adv. Nucl. Phys. **27**, 277 (2003), [hep-ph/0210398](#)
3. M.F.M. Lutz, E.E. Kolomeitsev, Nucl. Phys. **A730**, 392 (2004), [nucl-th/0307039](#)
4. M.F.M. Lutz, S. Leupold (2008), [arXiv: 0801.3821 \[nucl-th\]](#)
5. E.E. Jenkins, A.V. Manohar, M.B. Wise, Phys. Rev. Lett. **75**, 2272 (1995), [hep-ph/9506356](#)
6. G. Ecker, J. Gasser, A. Pich, E. de Rafael, Nucl. Phys. **B321**, 311 (1989)
7. G. Ecker, J. Gasser, H. Leutwyler, A. Pich, E. de Rafael, Phys. Lett. **B223**, 425 (1989)
8. P.D. Ruiz-Femenia, A. Pich, J. Portoles, JHEP **07**, 003 (2003), [hep-ph/0306157](#)
9. G. 't Hooft, Nucl. Phys. **B72**, 461 (1974)
10. W.M. Yao et al. (Particle Data Group), J. Phys. **G33**, 1 (2006)
11. B. Jongejans et al. (Amsterdam-CERN-Nijmegen-Oxford), Nucl. Phys. **B139**, 383 (1978)
12. F. Klingl, N. Kaiser, W. Weise, Z. Phys. **A356**, 193 (1996), [hep-ph/9607431](#)
13. D.H. Boal, B.J. Edwards, A.N. Kamal, R. Rockmore, R. Torgerson, Phys. Lett. **B66**, 165 (1977)
14. S. Okubo, Phys. Lett. **5**, 165 (1963)
15. G. Zweig, CERN Report No. 8419/TH-412 (1964)
16. J. Iizuka, Prog. Theor. Phys. Suppl. **37**, 21 (1966)
17. S. Leupold, M. Wagner (2008), [arXiv: 0807.2389 \[nucl-th\]](#)